Complementary Discrete Geometric *h*-Field Formulation for Wave Propagation Problems

Matteo Cicuttin[1], Lorenzo Codecasa[2], Ruben Specogna[1], and Francesco Trevisan[1]

[1]Dipartimento di Ingegneria Elettrica, Gestionale e Meccanica, Università degli Studi di Udine, Udine I-33100, Italy
[2]Dipartimento di Elettronica, Informazione e Bioingegneria, Politecnico di Milano, Milan I-20133, Italy

An electromagnetic wave propagation problem can be formulated according to a pair of complementary formulations, called the *e*-formulation and the *h*-formulation. The two formulations are linked to each other by Maxwell's curl equations, and, in the continuous setting, they are perfectly equivalent in describing the wave propagation phenomenon. However, this is not true in the discrete setting, where the two formulations, in general, give different solutions. In the past decades, complementary formulations were widely studied for static problems and eddy-current problems, where they were exploited as error estimators for adaptive refinement schemes. Moreover, the so-called bilateral energy bounds arise for some problems whether theoretically or at least numerically. However, to the best of our knowledge, little attention has been given to complementarity in the wave propagation problems. In this paper, we propose an adaptive refinement scheme using the constitutive error as an estimator, and then, we investigate the behavior in terms of bilateral energy bounds.

Index Terms— **Adaptive mesh refinement, complementarity, discrete geometric approach (DGA), finite integration technique, wave propagation.**

I. Introduction

An ELECTROMAGNETIC wave propagation problem is usually treated in terms of the electric field $\boldsymbol{e}$. In the framework of the discrete geometric approach (DGA) or finite integration technique [1]–[3], this leads to associate electric voltages to the edges of a primal simplicial grid and magnetomotive forces to the dual barycentric grid edges. However, it is well known that the electromagnetic problem can also be formulated in terms of the magnetic field $\boldsymbol{h}$. In the DGA, the solution of the discrete $\boldsymbol{h}$ problem can be obtained by swapping the role of the simplicial and barycentric grids, as it will be introduced in this paper.

In the past decades, a considerable effort has been expended in exploiting the complementarity of electromagnetic problems for a number of purposes, in particular for adaptive mesh refinement [4]–[6]. Notable results were obtained with static field problems, where bilateral energy bounds are established [7]. Moreover, a wide literature exists about complementarity in eddy-current problems. In this last class of problems, however, no energy bounds can be established, despite the fact that they are frequently observed in practical problems (see [8]). Complementarity in wave propagation problems seems to have received far less attention. To the best of our knowledge, it has been investigated only in [5] and [9]. In this paper, we investigated the topic using the two formulations to build an adaptive refinement scheme based on the approximation lying in the constitutive laws [5]. We then investigated the behavior in terms of bilateral energy bounds.

In Sections II and III, continuous- and discrete-wave propagation problems are introduced, both in the $\boldsymbol{e}$-formulation and the $\boldsymbol{h}$-formulation. The discrete $\boldsymbol{h}$-formulation is presented in Section IV. The impedance boundary condition (BC) is derived in Section IV-A. The adaptive mesh refinement algorithm is given in Section V. The numerical results are presented in Section VI. Finally, the conclusion is given in Section VII.

Manuscript received July 1, 2015; accepted August 20, 2015. Date of publication August 27, 2015; date of current version February 17, 2016. Corresponding author: M. Cicuttin (e-mail: matteo.cicuttin@uniud.it).

Color versions of one or more of the figures in this paper are available online at http://ieeexplore.ieee.org.

Digital Object Identifier 10.1109/TMAG.2015.2474162

II. Continuous-Wave Propagation Problem

From time-harmonic Maxwell's equations at an angular frequency ω in a bounded domain Ω

$$\nabla \times \boldsymbol{e} = -i\omega \boldsymbol{b}, \quad \nabla \times \boldsymbol{h} = i\omega \boldsymbol{d}$$

where $\boldsymbol{d}$, $\boldsymbol{e}$, $\boldsymbol{h}$, and $\boldsymbol{b}$ are, respectively, the electric displacement, electric, magnetic, and magnetic induction fields together with the constitutive relations

$$\boldsymbol{d} = \boldsymbol{\epsilon} \boldsymbol{e}, \quad \boldsymbol{h} = \boldsymbol{\nu} \boldsymbol{b}$$

where $\boldsymbol{\nu}$ and $\boldsymbol{\epsilon}$ are the symmetric positive definite material tensors, and the $\boldsymbol{e}$-formulation of the electromagnetic wave propagation problem

$$\nabla \times (\boldsymbol{\nu} \nabla \times \boldsymbol{e}) - \omega^2 \boldsymbol{\epsilon} \boldsymbol{e} = \boldsymbol{0} \tag{1}$$

can be derived [10]. Similarly, the $\boldsymbol{h}$-formulation of the electromagnetic problem becomes

$$\nabla \times (\boldsymbol{\xi} \nabla \times \boldsymbol{h}) - \omega^2 \boldsymbol{\mu} \boldsymbol{h} = \boldsymbol{0} \tag{2}$$

where $\boldsymbol{\xi} = \boldsymbol{\epsilon}^{-1}$ and $\boldsymbol{\mu} = \boldsymbol{\nu}^{-1}$.

Usual perfect electric conductor (PEC) ($\boldsymbol{n} \times \boldsymbol{e} = \boldsymbol{0}$) and perfect magnetic conductor (PMC) ($\boldsymbol{n} \times \boldsymbol{h} = \boldsymbol{0}$) BCs on $\partial\Omega$ with normal $\boldsymbol{n}$ can be applied to the wave propagation problems (1) and (2).

In the $\boldsymbol{e}$-formulation, the PEC is specified as a Dirichlet BC, while the PMC is a Neumann BC. In the $\boldsymbol{h}$-formulation, the opposite holds, that is, the PEC is specified as a Neumann condition, while the PMC is a Dirichlet condition [5]. Another BC of interest in the wave propagation problem is the impedance BC, used to constrain the electric and magnetic fields on a portion of $\partial\Omega$. The numerical treatment of this last condition, in the case of the $\boldsymbol{e}$-formulation, was already presented in [11] leading, by the energetic approach, to the admittance matrix $\mathbf{M}_Y$. However, the matrix $\mathbf{M}_Y$ is not suitable for the $\boldsymbol{h}$-formulation, so, in this paper, the impedance matrix $\mathbf{M}_Z$ will be derived, again by the energetic approach.

III. Discrete Counterpart of $\boldsymbol{e}$-Formulation

Numerical treatment of (1) requires the discretization of Ω, which is obtained by means of a primal tetrahedral grid $\mathcal{G}$ and a barycentric dual grid $\tilde{\mathcal{G}}$. The electromagnetic quantities are associated with these interlocked grids as follows:

1) electromotive force U_i to edges $e_i \in \mathcal{G}$;
2) magnetic flux Φ_i to faces $f_i \in \mathcal{G}$;
3) magnetomotive force F_i to edges $\tilde{e}_i \in \tilde{\mathcal{G}}$;
4) electric flux Ψ_i to faces $\tilde{f}_i \in \tilde{\mathcal{G}}$.

Problem (1) is discretized as [1], [2]

$$(\mathbf{C}^T\mathbf{M}_\nu\mathbf{C} - \omega^2\mathbf{M}_\epsilon)\mathbf{U} = \mathbf{0} \tag{3}$$

where $\mathbf{C}$ is the face-edge incidence matrix, $\mathbf{M}_\nu$ and $\mathbf{M}_\epsilon$ are the constitutive matrices obtained by the energetic approach described in [3], and $\mathbf{U}$ is the array of the unknown voltages along the primal edges. Introducing the impedance BCs, the problem

$$(\mathbf{C}^T\mathbf{M}_\nu\mathbf{C} - \omega^2\mathbf{M}_\epsilon)\mathbf{U} + i\omega\mathbf{M}_Y\mathbf{U} = -2i\omega\mathbf{F}^{b^-} \tag{4}$$

is obtained, where the term $\mathbf{F}^{b^-}$ represents an excitation applied to a portion of $\partial\Omega$ [2].

IV. Discrete Counterpart of $\boldsymbol{h}$-Formulation

The idea behind the complementary wave propagation problem is to exchange the roles of $\mathcal{G}$ and $\tilde{\mathcal{G}}$ by associating the following:

1) electromotive force U_i to edges $\tilde{e}_i \in \tilde{\mathcal{G}}$;
2) magnetic flux Φ_i to faces $\tilde{f}_i \in \tilde{\mathcal{G}}$;
3) magnetomotive force F_i to edges $e_i \in \mathcal{G}$;
4) electric flux Ψ_i to faces $f_i \in \mathcal{G}$.

In this way, the complementary discrete Maxwell equations are then written as

$$\mathbf{C}\mathbf{F} = i\omega\Psi \tag{5}$$
$$\mathbf{C}^T\mathbf{U} = -i\omega\Phi \tag{6}$$
$$\mathbf{U} = \mathbf{M}_\xi\Psi \tag{7}$$
$$\Phi = \mathbf{M}_\mu\mathbf{F}. \tag{8}$$

Solving (5) for Ψ and substituting it in (7) and then in (6), the complementary wave propagation problem results in being

$$(\mathbf{C}^T\mathbf{M}_\xi\mathbf{C} - \omega^2\mathbf{M}_\mu)\mathbf{F} = \mathbf{0} \tag{9}$$

where $\mathbf{M}_\xi$ and $\mathbf{M}_\mu$ are obtained by the energetic approach and represent the counterparts of $\mathbf{M}_\nu$ and $\mathbf{M}_\epsilon$, while $\mathbf{F}$ is the magnetomotive force along primal edges. Impedance BC and plane wave excitation can be introduced by adding two terms to (9), obtaining

$$(\mathbf{C}^T\mathbf{M}_\xi\mathbf{C} - \omega^2\mathbf{M}_\mu)\mathbf{F} + i\omega\mathbf{M}_Z\mathbf{F} = 2i\omega\mathbf{U}^{b^-} \tag{10}$$

where $\mathbf{U}^{b^-}$ is the excitation applied on a portion of $\partial\Omega$. Each nonzero entry of $\mathbf{U}^{b^-}$ corresponds to an edge of $\partial\Omega$. These entries are the voltages due to excitation along each edge of the portion of $\partial\Omega$ where excitation is applied.

A. Impedance Boundary Condition

At a boundary $\partial\Omega$ where an impedance BC is desired, the equation

$$Z(r)((\boldsymbol{n}\times\boldsymbol{h})\times\boldsymbol{n}) = \boldsymbol{n}\times\boldsymbol{e} \tag{11}$$

must hold. Moreover, for the properties of the boundary element basis functions $\boldsymbol{v}_i^{e^b}(\boldsymbol{r})$ [11], the equation

$$(\boldsymbol{n}\times\boldsymbol{h})\times\boldsymbol{n} = \sum_{i=0}^{\mathcal{E}}\boldsymbol{v}_i^{e^b}(\boldsymbol{r})F_i^b \tag{12}$$

holds.

B. Constitutive Matrix $\mathbf{M}_Z$

The constitutive impedance matrix $\mathbf{M}_Z$ is obtained by the energetic approach [3], [12] in a similar way as done for $\mathbf{M}_Y$ in [11]. Let $\boldsymbol{e}'$ and $\boldsymbol{h}$ be two independent fields. We compute the flux of the vector $\boldsymbol{e}'\times\boldsymbol{h}$ across the surface $\partial\Omega$

$$\begin{aligned}\int_{\partial\Omega}\boldsymbol{e}'\times\boldsymbol{h}^*\cdot\boldsymbol{n}ds &= \int_{\partial\Omega}\boldsymbol{n}\times\boldsymbol{e}'\cdot\boldsymbol{h}^*ds\\ &= \int_{\partial\Omega}(\boldsymbol{n}\times\boldsymbol{e}')\cdot((\boldsymbol{n}\times\boldsymbol{h})\times\boldsymbol{n})^*ds\\ &= \int_{\partial\Omega}(\boldsymbol{n}\times\boldsymbol{e}')\cdot\left(\sum_{i=0}^{\mathcal{E}}\boldsymbol{v}_i^{e^b}(\boldsymbol{r})F_i^b\right)^*ds\\ &= \sum_{i=0}^{\mathcal{E}}F_i^{b^*}\int_{\partial\Omega}(\boldsymbol{n}\times\boldsymbol{e}')\cdot\boldsymbol{v}_i^{e^b}(\boldsymbol{r})ds\\ &= \sum_{i=0}^{\mathcal{E}}F_i^{b^*}\int_{\partial\Omega}\left(\boldsymbol{v}_i^{e^b}(\boldsymbol{r})\times\boldsymbol{n}\right)\cdot\boldsymbol{e}'ds\\ &= -\sum_{i=0}^{\mathcal{E}}F_i^{b^*}\int_{\partial\Omega}\left(\boldsymbol{n}\times\boldsymbol{v}_i^{e^b}(\boldsymbol{r})\right)\cdot\boldsymbol{e}'ds\\ &= -\sum_{i=0}^{\mathcal{E}}F_i^{b^*}\sum_{j=0}^{\mathcal{F}}\int_{f_j^b}\left(\boldsymbol{n}\times\boldsymbol{v}_i^{e^b}(\boldsymbol{r})\right)\cdot\boldsymbol{e}'ds\\ &= -\sum_{i=0}^{\mathcal{E}}F_i^{b^*}U_i^b = -\boldsymbol{F}^{b'^H}\boldsymbol{U}^{b'}.\end{aligned} \tag{13}$$

Because of (11) and (12)

$$\int_{\partial\Omega}\boldsymbol{e}'\times\boldsymbol{h}^*\cdot\boldsymbol{n}ds \tag{14}$$
$$= \int_{\partial\Omega}\left(Z(\boldsymbol{r})\sum_{i=0}^{\mathcal{E}}\boldsymbol{v}_i^{e^b}(\boldsymbol{r})F_i^b\right)\left(\sum_{j=0}^{\mathcal{E}}\boldsymbol{v}_j^{e^b}(\boldsymbol{r})F_j^b\right)^* \tag{15}$$
$$= \boldsymbol{F}^{b^H}(\mathbf{M}_Z\boldsymbol{F}^b) \tag{16}$$

so $\boldsymbol{U}^b = -\mathbf{M}_Z\boldsymbol{F}^b$ holds, see Fig. 1. The entries of the impedance matrix are then calculated as

$$(\mathbf{M}_Z)_{ij} = \int_{\partial\Omega}Z(\boldsymbol{r})\left(\boldsymbol{v}_i^{e^b}(\boldsymbol{r})\cdot\boldsymbol{v}_j^{e^b}(\boldsymbol{r})\right)ds. \tag{17}$$

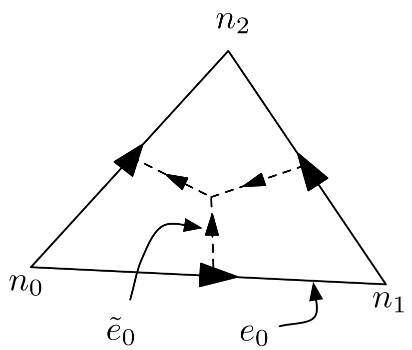

Fig. 1. Orientation of the edges on a boundary $\partial\Omega$. When $\boldsymbol{e}$ is associated with primal edges and $\boldsymbol{h}$ to the dual edges, $e_i^b \times \tilde{e}_i^b$ and $\boldsymbol{e} \times \boldsymbol{h}$ have the same orientation. Swapping the grids $e_i^b \times \tilde{e}_i^b$ has the orientation of $\boldsymbol{h} \times \boldsymbol{e} = -(\boldsymbol{e} \times \boldsymbol{h})$.

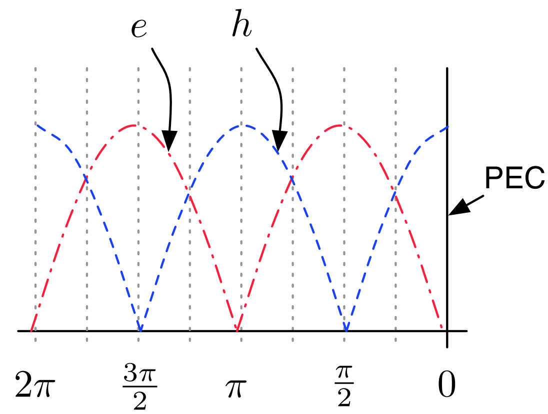

Fig. 2. Standing wave that forms when a plane wave hits a PEC wall. If magnetic field is the quantity of interest, refinement should be done around $(\pi/2)$ and $(3\pi/2)$, where the field variations are higher. Electric field, however, would require maximal refinement around 0, π, and 2π. Thus, setting $\delta = 0.5$ would lead to a rather uniform refinement, while setting $\delta = 0$ or $\delta = 1$ will favor the magnetic field or electric field, respectively.

V. Adaptive Mesh Refinement

It is a known fact that, in the discrete domain, constitutive laws are approximated, and thus, $\boldsymbol{b}$ is not equal to $\boldsymbol{\mu h}$, as well as $\boldsymbol{d}$ is not equal to $\boldsymbol{\epsilon e}$. For this reason, as already noted by Bossavit, this *"inconsistency in the constitutive laws can be used as an error estimator"* [5]. Thus, we propose an adaptive mesh refinement scheme based on the comparison of the electromagnetic energies calculated from the $\boldsymbol{e}$-formulation and the $\boldsymbol{h}$-formulation. The main idea behind the scheme is to refine the mesh in the subregions of Ω, where the relative error between the calculated energies is maximal (Fig. 4), since *"the subdivision of the guilty elements and their neighbors cannot fail to improve the result"* [9, pp. 336–337]. The entire idea can be summarized in the following iterative procedure.

1) Solve problems (4) and (10).
2) Interpolate the fields in the mesh volumes v_i with piecewise constant basis functions [3], obtaining:
   a) primal fields $\boldsymbol{e}_{p,i}$, $\boldsymbol{h}_{p,i}$;
   b) dual fields $\boldsymbol{e}_{d,i}$ and $\boldsymbol{h}_{d,i}$.
3) For each v_i, let:
   a) $\Delta\boldsymbol{e}_i = \boldsymbol{e}_{p,i} - \boldsymbol{e}_{d,i}$;
   b) $\Delta\boldsymbol{h}_i = \boldsymbol{h}_{p,i} - \boldsymbol{h}_{d,i}$;

   and then compute

$$\Delta w_i = \delta \int_{v_i} \Delta\boldsymbol{e}_i \cdot \epsilon \Delta\boldsymbol{e}_i \, dv \tag{18}$$

$$+(1-\delta) \int_{v_i} \Delta\boldsymbol{h}_i \cdot \mu \Delta\boldsymbol{h}_i \, dv. \tag{19}$$

   The quantity Δw_i represents the absolute energy error between the two formulations in the ith element, while δ is a coefficient in range $[0, \ldots, 1]$.
4) Let $\mathcal{T}$ be the set of the tetrahedra in which Ω is discretized:
   a) compute

$$w_{p,i} = \delta \int_{v_i} \boldsymbol{e}_{p,i} \cdot \epsilon \boldsymbol{e}_{p,i} \, dv + (1-\delta) \int_{v_i} \boldsymbol{h}_{p,i} \cdot \mu \boldsymbol{h}_{p,i} \, dv.$$

   b) compute the relative error $\eta(t) = \Delta w_i / w_{p,i}$ for each $v_i \in \mathcal{T}$.
5) Assign the tetrahedra of Ω to two sets $\mathcal{T}_h$ and $\mathcal{T}_l$, where the first set contains the $k \cdot 100\%$ of the tetrahedra and maximizes the error, while the second set contains the other tetrahedra. Otherwise let $k \in [0, 1]$ and $\eta(\mathcal{X}) = \sum_{x \in \mathcal{X}} \eta(x)$:
   a) make a set $\mathcal{T}_h \subset \mathcal{T}$, such that $\text{card}(\mathcal{T}_h) = k \cdot \text{card}(\mathcal{T})$ and $\eta(\mathcal{T}_h)$ is maximized;
   b) make a set $\mathcal{T}_l = \mathcal{T} \setminus \mathcal{T}_h$ that contains the remaining tetrahedra.
6) For each tetrahedron $v_i \in \mathcal{T}_h$, divide its radius by r_h.
7) For each tetrahedron $v_i \in \mathcal{T}_l$, divide its radius by r_l.

Good results were obtained by setting $k = 0.1$, $r_h = 3$, and $r_l = 1.2$. The error weighting coefficient δ is used to privilege the magnetic energy error ($\delta = 1$) or the electric energy error ($\delta = 0$) in the refinement process. In the first case, the refinement captures the rapid variations of $\boldsymbol{e}$, while in the second case, the rapid variations of $\boldsymbol{h}$. This could be useful in some cases, for example, in the presence of strong standing waves (Fig. 2).

VI. Numerical Results

We numerically investigated, for a number of wave propagation problems, the convergence behavior of the two formulations by calculating some energetic quantities at each refinement step, specifically the electric energy [12]

$$w_e = \frac{1}{4} \int_\Omega \epsilon |\boldsymbol{e}|^2 dv \tag{20}$$

and the magnetic energy [12]

$$w_m = \frac{1}{4} \int_\Omega \mu |\boldsymbol{h}|^2 dv. \tag{21}$$

As an example (Fig. 3), the electric energy of a plane wave traveling in a box of 1 m × 1 m × 1 m and with an interface $\Gamma = 0.25$ at the end was calculated. At the second step, the refinement procedure produced a mesh of ∼8000 elements in the cases $\delta = 0$ and $\delta = 1$, while it produced a mesh

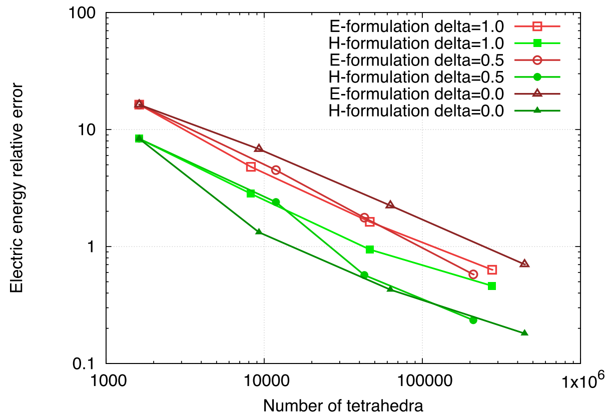

Fig. 3. Comparison of electric energy convergence of the two formulations using different error weighting coefficients: number of tetrahedra versus absolute energy error. The expected electric energy value is $w_e = 2.35 \times 10^{-12}$ J.

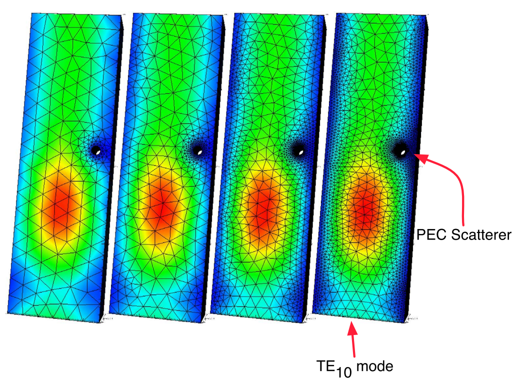

Fig. 4. Four steps of adaptive mesh refinement on a section of rectangular waveguide excited with TE_{10} mode and a scatterer inside. Parameters used are $r_h = 3, r_l = 1.2$, and $\delta = 1$. The adaptive scheme correctly refines the mesh near boundaries, where the variation of the field is higher.

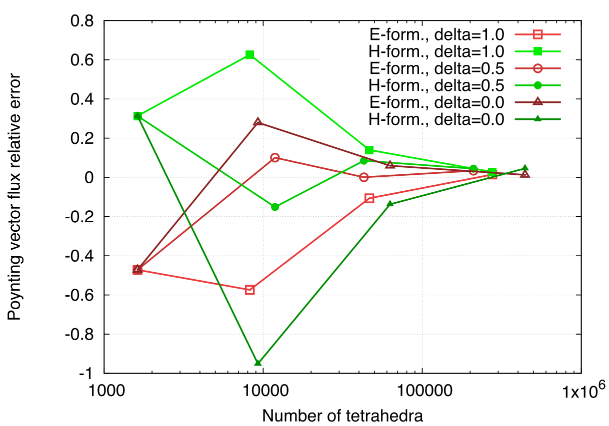

Fig. 5. Comparison of Poynting vector flux convergence of the two formulations using different error weighting coefficients: number of tetrahedra versus absolute flux error. The expected power flowing across $\partial\Omega$ is 1.244×10^{-3} W.

of ~12 000 elements with $\delta = 0.5$ (uniform refinement). In the case where $\delta = 1$, we observed almost the same accuracy of the case $\delta = 0.5$, despite a 33% reduction of the number of elements (Fig. 3). At the third step, the procedure produced a mesh of ~44 000 elements in the cases where $\delta = 1$ and $\delta = 0.5$, while it produced a mesh of ~62 000 elements in the case $\delta = 0$; with equal number of elements, the refinement based on electric energy error is slightly more precise than the uniform refinement. Such a test problem was chosen to have analytical expressions for the energetic quantities; however, the same behavior was observed in more complex problems, as, for example, in waveguides with scattering objects inside (Fig. 4), thus suggesting some effectiveness of the proposed technique. Energetic quantities across the domain boundaries were also calculated, despite the calculation converges to the correct value, but inconclusive results were obtained (Fig. 5).

VII. Conclusion

The discrete complementary formulation of the wave propagation problem was presented, and an adaptive mesh refinement scheme was devised. Bilateral convergence of energetic quantities was also investigated. In the various problems we solved, no bilateral energy bounds were observed, as instead happens in static problems or in eddy-current problems [8].

Acknowledgment

This work was supported by the PAR-FSC 2013 EMCY Project of the Friuli Venezia Giulia region.

References

[1] M. Clemens and T. Weiland, "Discrete electromagnetism with the finite integration technique," *Prog. Electromagn. Res.*, vol. 32, pp. 65–87, 2001.

[2] S. Chialina, M. Cicuttin, L. Codecasa, R. Specogna, and F. Trevisan, "Plane wave excitation for frequency domain electromagnetic problems by means of impedance boundary condition," *IEEE Trans. Magn.*, vol. 51, no. 3, Mar. 2015, Art. ID 7203504.

[3] L. Codecasa, R. Specogna, and F. Trevisan, "Symmetric positive-definite constitutive matrices for discrete eddy-current problems," *IEEE Trans. Magn.*, vol. 43, no. 2, pp. 510–515, Feb. 2007.

[4] J. Rikabi, C. F. Bryant, and E. M. Freeman, "An error-based approach to complementary formulations of static field solutions," *Int. J. Numer. Methods Eng.*, vol. 26, no. 9, pp. 1963–1987, Sep. 2005.

[5] N. A. Golias, T. D. Tsiboukis, and A. Bossavit, "Constitutive inconsistency: Rigorous solution of Maxwell equations based on a dual approach," *IEEE Trans. Magn.*, vol. 30, no. 5, pp. 3586–3589, Sep. 1994.

[6] R. Specogna, "Extraction of VLSI multiconductor transmission line parameters by complementarity," *IEEE Trans. Very Large Scale Integr. (VLSI) Syst.*, vol. 22, no. 1, pp. 146–154, Jan. 2014.

[7] J. L. Synge, *The Hypercircle in Mathematical Physics*. Cambridge, U.K.: Cambridge Univ. Press, 1957.

[8] Z. Ren and H. Qu, "Investigation of the complementarity of dual eddy current formulations on dual meshes," *IEEE Trans. Magn.*, vol. 46, no. 8, pp. 3161–3164, Aug. 2010.

[9] A. Bossavit, *Computational Electromagnetism: Variational Formulations, Complementarity, Edge Elements*. London, U.K.: Academic, 1998.

[10] R. E. Collin, *Foundations for Microwave Engineering*, 2nd ed. New York, NY, USA: McGraw-Hill, 1992.

[11] L. Codecasa, R. Specogna, and F. Trevisan, "Discrete geometric formulation of admittance boundary conditions for frequency domain problems over tetrahedral dual grids," *IEEE Trans. Antennas Propag.*, vol. 60, no. 8, pp. 3998–4002, Aug. 2012.

[12] L. Codecasa and F. Trevisan, "Piecewise uniform bases and energetic approach for discrete constitutive matrices in electromagnetic problems," *Int. J. Numer. Methods Eng.*, vol. 65, no. 4, pp. 548–565, 2006.